International Journal of Computational and Experimental Science and ENgineering (IJCESEN)

Vol. 11-No.4 (2025) pp. 9933-9940
http://www.ijcesen.com

ISSN: 2149-9144

Research Article

Mapping the vulnerability to surface-water pollution of Sebkhet El Mellah (El-Meniaa, Algeria)

Meriem Oulad Heddar[1], Mohamed Kraimat[2]*, Cherifa Djaaroune[3], Om Keltoum Oulad Hadj Youcef[4], Samia Bissati[5]

[1] Département de Biologie, Faculté des Sciences de la Nature et de la Vie et Sciences de la Terre, Université de Ghardaïa, 47000, Algeria
Email: ouladheddar.meriem@univ-ghardaia.dz - **ORCID:** 0009-0005-4640-8719

[2] Laboratoire de Valorisation et de Conservation des Ecosystèmes Arides, Université de Ghardaïa, 47000, Algeria
* **Corresponding Author Email:** kraimat.mohamed@univ-ghardaia.dz - **ORCID:** 0000-0002-3240-5868

[3]Département de Biologie, Faculté des Sciences de la Nature et de la Vie et Sciences de la Terre, Université de Ghardaïa, 47000, Algeria
Email: cherif2a@gmail.com - **ORCID:** 0009-0005-0040-8719

[4]Département de Biologie, Faculté des Sciences de la Nature et de la Vie et Sciences de la Terre, Université de Ghardaïa, 47000, Algeria
Email: had2i@gmail.com - **ORCID:** 0009-0005-4330-8719

[5]Laboratoire Bioressources Sahariennes, Université Kasdi Merbah, Ouargla, 30000, Algeria
Email: bissati.samia@univ-ouargla.dz - **ORCID:** 0000-0002-0285-0274

Article Info:

DOI: 10.22399/ijcesen.4560
Received: 15 June 2025
Revised: 22 November 2025
Accepted: 10 December 2025

Keywords

Mapping
Vulnerability
Surface-water
Wetland
Variability

Abstract:

Sebkhet El Mellah, located in the El Meniaa region in central Algeria, is an endorheic Saharan wetland designated as a Ramsar site (site no. 1429) since 12 December 2004 and covering 18947 ha. Despite its ecological importance, the lake system is exposed to increasing anthropogenic pressures in an arid environment where short-lived runoff events can rapidly transfer pollutants into closed basins. This study develops a GIS-based surface-water pollution vulnerability map for Sebkhet El Mellah by integrating a geostatistical method. 35 samples were prospected for in-situ measurements (pH, electrical conductivity (EC), total dissolved solids (TDS), and dissolved oxygen (DO)) utilizing the portable instruments. Turbidity was measured with a formazin-calibrated turbidimeter and reported as nephelometric turbidity units (NTU). Dissolved inorganic characteristics (nitrate (NO_3^-), ammonium (NH_4^+), and orthophosphate (PO_4^{3-})) were quantified by standard UV–Vis colorimetric methods. The results obtained showed that Electrical conductivity (EC) and total dissolved solids (TDS) have a substantial positive connection ($R= 0.99$, $p< 0.001$). Turbidity demonstrates a notable positive connection with PO_4^{3-} ($R= 0.55$, $p< 0.01$). NH_4^+ exhibited a significant correlation with DO ($R= 0.72$, $p< 0.001$), but with marginally reduced contributions from Dim1. Turbidity exhibits negative correlations with dissolved oxygen (DO) ($R = -0.59$, $p< 0.01$) and nitrate (NO_3^-) ($R = -0.45$, $p< 0.05$). The analytical method used in this study serves as an effective tool for pinpointing sensitive regions and facilitating the sustainable management of wetland ecosystems in arid areas.

1. Introduction

Wetlands provide essential ecosystem services, including water storage, groundwater recharge or discharge regulation, nutrient retention, carbon cycling, biodiversity support, and climate moderation [1]. These functions are especially vital in arid and hyper-arid environments, where wetland systems may serve as scarce and spatially constrained refuges for aquatic and semi-aquatic species, as well as for human activities reliant on oasis landscapes [2,3]. However, arid-zone wetlands are often highly vulnerable to environmental degradation because their hydrology relies on

sporadic rainfall and transient runoff events [4]. Additionally, elevated evaporation rates and restricted dilution capacity can enhance the persistence and concentration of dissolved constituents. In endorheic basins, where water and solutes accumulate instead of being exported downstream, the sensitivity to pollution inputs may be heightened [5-7].Sebkhet El Mellah, located in the El Menia (El-Menea) region of central Algeria, is a Saharan salt-lake system characterized by episodic surface inflows and strong salinity gradients [8]. Like many salt-lake wetlands, its ecological functioning is controlled by the balance between occasional inflows through wadis or local drainage pathways and intense evaporative losses. The site is important for the conservation of Mediterranean and Central Saharan biodiversity due to its habitat diversity, notably tamarisk populations and dunes that host a range of species: reptiles, amphibians, algae, phanerogams, fish, crustaceans, birds, and small mammals. The region's high productivity, favored by high temperatures and, consequently, a high decomposition rate, makes it a nesting and breeding site for several species of waterfowl, including more than 1% of the biogeographic populations of the ruddy shelduck (*Tadorna ferruginea*) and the ferruginous duck (*Aythya nyroca*). More than 110 avifauna species, belonging to 30 families with very different ecological requirements, have been recorded [9]. Ancient burials are found in the region, while the cliffs harbor marine paleontological remains. Human pressures in Saharan towns and oasis environments may exacerbate risks to adjacent wetlands. The expansion of settlements, agricultural intensification through the use of fertilizers, pesticides, and irrigation return flows, unregulated solid waste disposal, and inadequately treated or untreated wastewater contribute to various pollution pathways. The intersection of these pressures with hydrological connectivity, especially in drainage channels, wadis, and low-slope convergent terrain, can lead to spatial concentration of surface-water pollution risks [10, 11].Vulnerability mapping offers an effective, practical way to pinpoint areas where surface-water pollution is likely to affect a wetland, particularly when monitoring data is scarce. In this context, vulnerability is defined as a synthesis of pollution pressure, which includes the presence and intensity of sources, and environmental susceptibility, characterized by factors such as terrain, land cover, and hydrological connectivity that influence transport and accumulation [12].This study develops a GIS-based surface-water pollution vulnerability map for Sebkhet El Mellah by integrating physicochemical and pollution parameters. The resulting vulnerability classes are evaluated using targeted field measurements of physicochemical water-quality indicators at representative sites and hydrological conditions. The objectives are to highlight the current state of the physicochemical quality of Sebkhet El Mellah's waters and to map their spatial variability. The outputs aim to guide efficient monitoring design and support locally relevant catchment and wetland protection actions.

2. Material and methods

2.1 Water sampling design

Sampling was conducted using a random design during a dry period in 2023 to capture the pulse-driven dynamics typical of arid endorheic systems. Surface-water samples were collected from Sebkhet El Mellah at 35 points, with 3 replicates per sampling point. Site coordinates were documented using a handheld GPS in the UTM WGS 84 projection system (Figure 1). Water was collected from 10–20 cm below the surface into pre-cleaned polyethylene bottles. Samples intended for dissolved nutrient determinations (nitrate, nitrite, and orthophosphate) were filtered through 0.45 µm membrane filters to obtain the dissolved fraction and reduce interferences from suspended solids. All samples were stored in the dark in an insulated cooler and transported to the laboratory under refrigerated conditions (4 °C).

2.2 In situ measurements

Physicochemical parameters were assessed in situ utilizing portable meters. The pH was measured with a calibrated pH electrode, using a two-point calibration with standard buffers suitable for the anticipated pH range [13]. Electrical conductivity (EC) was assessed with temperature compensation activated and calibrated utilizing conductivity standards. Total dissolved solids (TDS) were calculated using electrical conductivity (EC) utilizing the meter's conversion factor, while water temperature was recorded concurrently [14]. Dissolved oxygen (DO) was measured in situ with a portable DO meter, calibrated to air saturation according to the manufacturer's instructions; measurements were documented after stabilization, employing moderate probe movement to prevent boundary-layer effects [15].

2.3 Laboratory analysis of pollution indicators

Turbidity was determined using a turbidimeter calibrated with formazin standards and reported in

nephelometric turbidity units (NTU). Samples were gently inverted to homogenize without introducing bubbles, transferred to clean cuvettes, and measured after visual inspection for bubbles and removal of external droplets. When turbidity exceeded the instrument's linear range, appropriate dilutions were performed, and the dilution factor was applied [16].

The dissolved inorganic parameters were evaluated using standard colorimetric methods and a UV-Vis spectrophotometer. A validated reduction-based colorimetric process was used to measure nitrate (NO_3^-), ammonium (NH_4^+) was determined using the phenate (indophenol blue/Berthelot) reaction,

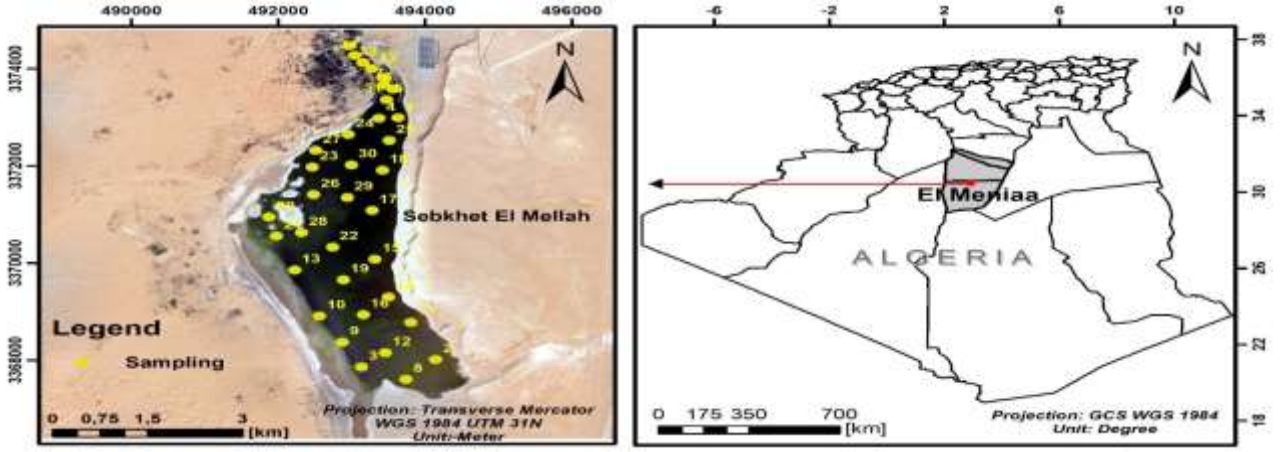

Figure 1. *Map of study area (Sebkhet El Mellah) surface-water sampling*

following an established standard protocol, and orthophosphate (PO_4^{3-}) using the molybdenum blue (ascorbic acid) method following color development [17].

2.4 Statistical and geostatistical analyses

Variability maps were produced through auto-kriging settings in R 4.5.1, employing an automated function (*autoKrige*) to determine optimal variogram parameters and perform kriging interpolation. After selecting the optimal model, the software performs kriging interpolation to estimate values at unmeasured locations, and the resulting estimates are used to generate thematic maps in QGIS 3.34.9. Thus, a Principal Component Analysis (PCA-biplot) and a multiple correlation matrix were generated according to the Pearson method using the *corrplot* function to identify the most significant associations.

3. Results and Discussions

3.1 Physicochemical characteristics of surface-water

Figure 2 presents box-and-whisker plots summarizing the distribution of the physicochemical water quality parameters. The pH values show an even tighter distribution, with minimal dispersion around 6.51 ± 0.64 [-], reflecting stable acid–base conditions. The stability of pH, in particular, implies well-buffered conditions, which may reflect consistent geochemical controls or limited external inputs affecting acidity or alkalinity. EC and TDS exhibit relatively fickle ionic composition and dissolved load, suggesting greater fluctuations in salinity or mineral inputs, with values of 3.36 ± 2.21 [mS/cm] and 1.85 ± 1.31 [mg/L], respectively. In contrast, turbidity shows a substantially wider interquartile range and extended whiskers (25.55 ± 21.73 [NTU]), indicating pronounced variability among samples.

3.2 Pollution indicators

DO concentrations exhibit important variability, with values distributed around 1.26 ± 1.4 [mg/L]. NO_3^- concentrations are comparatively low and narrowly distributed, with a small interquartile range and limited spread (0.44 ± 0.44 [mg/L]). PO_4^{3-} values show significant variability, with a distribution broader than 0.66 ± 0.49 [mg/L]. NH_4^+ shows the lowest spread among the parameters, characterized by a narrow interquartile range and a short upper whisker (0.21 ± 0.06 [mg/L]) (Figure 3).

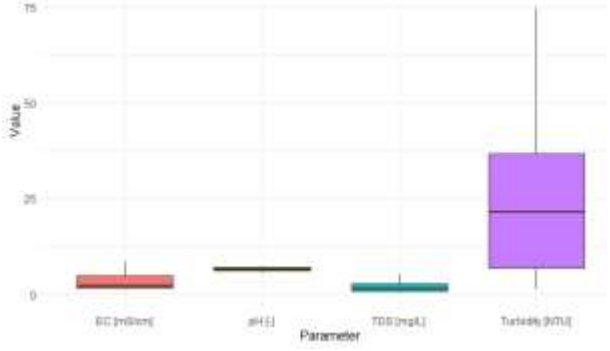

Figure 2. *Variation of physicochemical properties of surface-water*

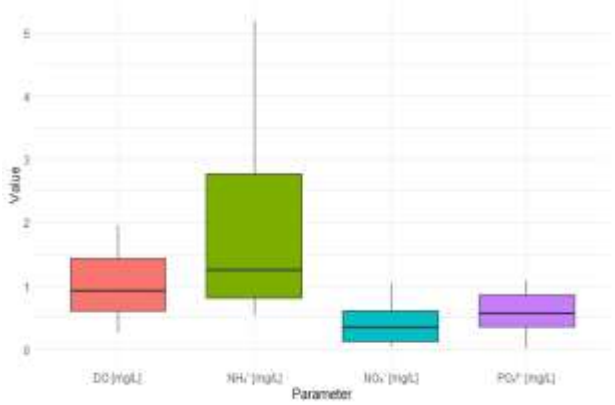

Figure 3. *Variation of pollution indicators of surface-water*

3.3 Spatial distribution

The pH map indicates values between 5.81 and 7.01, with minimal variability (CV = 9.83%). Lower pH values are predominantly found in the middle and northern areas of the study wetland, whereas higher pH values are observed in the southern region. EC exhibits significant variability (CV =65.77%), with spatial values ranging from 1.62 [mS/cm] to 5.33 [mS/cm]. Elevated EC zones are prominent in the northern and southern extremes, while lower values predominate in the core region. A comparable regional distribution of TDS is observed, ranging from 0.84 mg/L to 2.87 mg/L, with elevated concentrations in the southern region and somewhat lower values in the central zone (CV = 70.81%). Turbidity shows the greatest spatial variability among the metrics, with values ranging from 1.42 [NTU] to 89.84 [NTU]. Localized hotspots of elevated turbidity are evident, especially in the southern and northeastern areas, although reduced turbidity values are more prevalent throughout the center region (Table 1).

DO concentrations range from 1.01 [mg/L] to 34.98 [mg/L], showing a clear spatial gradient with lower DO values concentrated in the northern sector and progressively higher concentrations toward the southern region (CV = 82.54%). NO_3^- varies between 0.04 [mg/L] and 2.10 [mg/L] and exhibits distinct localized hotspots, particularly in the central and western parts of the study area, while lower concentrations dominate the southern sector. PO_4^{3-} ranges from 0.01 [mg/L] to 1.90 [mg/L] and displays pronounced spatial heterogeneity (CV=74.24%), with elevated values observed mainly in the southern and central zones. However, NH_4^+ concentrations oscillate between 0.15 [mg/L] and 0.44 [mg/L], characterized by localized enrichment zones in the central portion of the study area, while lower concentrations are more widely distributed elsewhere (Table 2) (Figure 4).

3.4 Multivariate analysis

Principal Component Analysis (PCA-biplot) was applied to explore relationships among physicochemical and pollution indicators and to identify the dominant factors controlling water quality variability. The first principal component (Dim1) explains 31.9% of the total variance, while the second principal component (Dim2) accounts for 22.4%, together explaining 54.3% of the overall data variability (Figure 5). EC and TDS show significant positive correlation (R= 0.99, p< 0.001). Turbidity exhibits a significant positive correlation with PO_4^{3-} (R= 0.55, p< 0.01). NH_4^+ was also positively associated with DO (R= 0.72, p< 0.001), though with slightly lower contributions from Dim1. In contrast, turbidity shows negative associations with DO (R = -0.59, p< 0.01) and NO_3^- (R = -0.45, p< 0.05) (Figure 6).

Table 1. *Fitted variogram models and variation properties.*

Parameter	Model	Nugget	Sill	Range
pH [-]	Exponential	0.46	0.87	4693
EC [mS/cm]	Exponential	4.6	4.7	3032
Turbidity [NTU]	Spherical	424	513	349
TDS [mg/L]	Spherical	1.6	1.6	3360
DO [mg/L]	Gaussian	0	1.2	332
NO_3^- [mg/L]	Gaussian	0	0.2	382
NH_4^+ [mg/L]	Gaussian	0	0	406
PO_4^{3-} [mg/L]	Gaussian	0.31	0.31	724

Table 2. *Statistical data of physicochemical properties and pollution indicators.*

Parameter	Mean	SD	CV (%)
pH [-]	6.51	0.64	9.83
EC [mS/cm]	3.36	2.21	65.77
Turbidity [NTU]	25.55	21.73	85.05
TDS [mg/L]	1.85	1.31	70.81
DO [mg/L]	1.26	1.04	82.54
NO_3^- [mg/L]	0.44	0.44	100
NH_4^+ [mg/L]	0.21	0.06	28.57
PO_4^{3-} [mg/L]	0.66	0.49	74.24

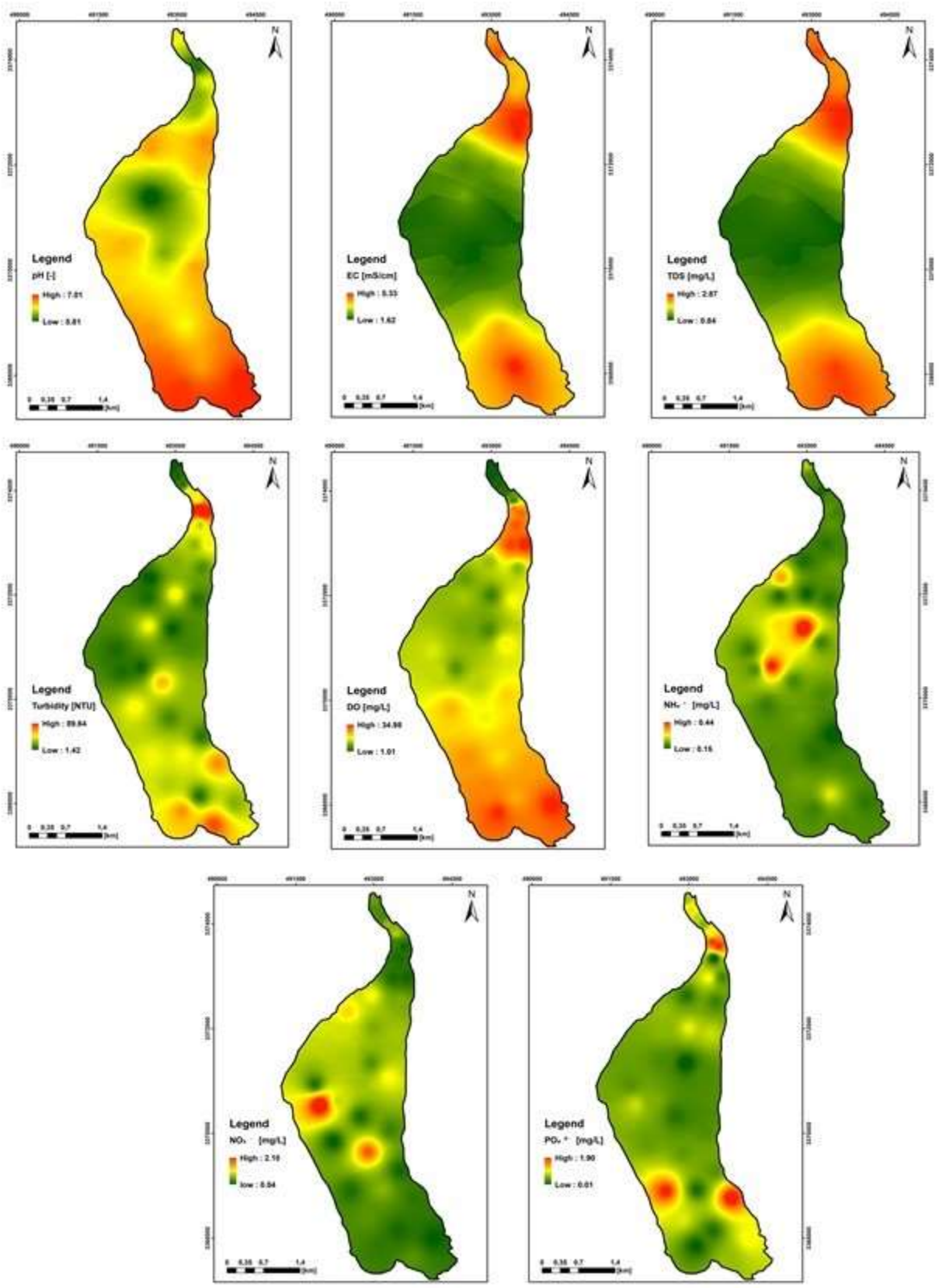

Figure 4. *Spatial variability of physicochemical properties and pollution indicators of surface-water*

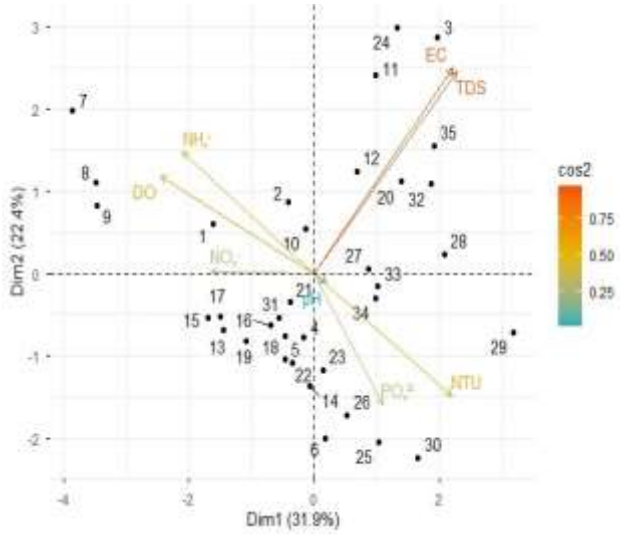

Figure 5. *PCA-biplot illustrating the contributions of variables*

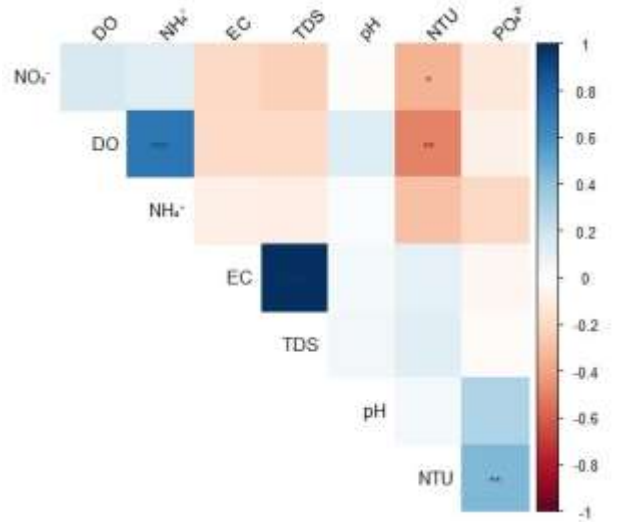

Figure 6. *Corrplot illustrating the correlations between surface-water variables*

4. Conclusions

The present study evaluated the vulnerability of surface waters in Sebkhet El Mellah (El-Meniaa, Algeria) to pollution using an integrated approach combining physicochemical and nutrient analyses, spatial interpolation, and multivariate statistical methods. The results reveal marked spatial heterogeneity in water quality, reflecting the combined influence of mineralization processes, hydrological conditions, and localized pollution inputs. Physicochemical parameters such as electrical conductivity, total dissolved solids, and pH exhibit clear spatial gradients, indicating variable mineralization and evaporative concentration across the wetland. In contrast, pollution indicators, including turbidity, ammonium, nitrate, and phosphate, display localized hotspots, suggesting point-scale enrichment and dynamic biogeochemical processes. Multivariate analyses highlight two dominant controlling factors: (i) mineralization and particulate enrichment, represented by strong associations among EC, TDS, turbidity, and orthophosphate; and (ii) oxygen–nutrient dynamics, reflected by the relationships between dissolved oxygen and nitrogen species. The negative correlation between dissolved oxygen and turbidity, together with the spatial decoupling of ammonium and nitrate, suggests non-equilibrium nitrogen cycling under variable redox conditions. Future research should focus on long-term monitoring, integrating land-use and hydrological data, and assessing ecological responses to changes in water quality. The methodological framework applied in this work provides a useful tool for identifying vulnerable areas and supporting sustainable management of wetland ecosystems in arid environments.

Author Statements:

- **Ethical approval:** The conducted research is not related to either human or animal use.
- **Conflict of interest:** The authors declare that they have no known competing financial interests or personal relationships that could have appeared to influence the work reported in this paper
- **Acknowledgement:** The authors are grateful to the LVCEA—Valorization and Conservation of Arid Ecosystems Laboratory, University of Ghardaïa, Algeria, for supporting this research study.
- **Author contributions:** The authors declare that they have equal right on this paper.
- **Funding information:** The authors declare that there is no funding to be acknowledged.
- **Data availability statement:** The data that support the findings of this study are available on request from the corresponding author. The data are not publicly available due to privacy or ethical restrictions.

References

[1] Qi, Q., Wang, Z., Zhang, Z. (2025). Construction and application of copula-based trivariate standardized river disconnection index for seasonal rivers in arid and semi-arid areas. Sci Rep. 15, 26621. https://doi.org/10.1038/s41598-025-11513-w.

[2] Choutri, I., Hussien, A. (2024). Exploratory analysis of Algeria meteorological drought using SPI and SPEI". oalib, 11(3), 1–25. https://doi.org/10.4236/oalib.1111897.

[3] Sennour, K., Chiali-Charif, K., Boucetta, S., Benabi, F. & Kerfouf, A. (2026). Diversity and community

structure of microalgae and cyanobacteria in Oglat Eddaira Wetland (South-Western Algeria). Journal of Ecological Engineering, 27(2).

[4] Zhang, D., Hu, B., Chen, L., Qi, P., Wu, Y., Liu, X., Zhang, G., Zhang, W. (2024). Spatiotemporal variation of water level in wetlands based on multi-source remote sensing data and responses to changing environments. Sci Total Environ, 955:177060. https://doi.org/10.1016/j.scitotenv.2024.177060.

[5] Ding, Y., Ding, J., Wang, J., Han, L., Wang, J., Chen, X., Ge, X. (2025). Spatiotemporal dynamics and driving mechanisms of wetlands in arid regions of Xinjiang. Ecol Indic, 174, 113485. https://doi.org/10.1016/j.ecolind.2025.113485.

[6] Hammana, C., Pereña-Ortiz, J.F., Meddad-Hamza, A., Hamel, T., Salvo-Tierra, Á.E. (2024). The Wetlands of Northeastern Algeria (Guelma and Souk Ahras): Stakes for the conservation of regional biodiversity. Land, 13, 210. https://doi.org/10.3390/land13020210.

[7] Kerns, B.W., Chen, S.S. (2021). Impacts of precipitation–evaporation–salinity coupling on upper ocean stratification and momentum over the tropical pacific prior to onset of the 2018 El Niño. Ocean Modelling, 168, 101892. https://doi.org/10.1016/j.ocemod.2021.101892.

[8] Ouldjaoui, M. ., Hassad, S. ., Dib, D. ., & Houha, B. . (2023). Hydrogeochemistryof groundwater in Es-Sbikhat El-Mahmel basin, Khenchela (NE Algeria). Journal of Fundamental and Applied Sciences, 12(2), 800–813. https://doi.org/10.4314/jfas.v12i2.18

[9] Chedad, A., Bendjoudi, D., Guezoul, O. (2020). Biodiversité de l'avifaune aquatique d'une zone humide artificielle à Kef Doukhane (Ghardaia, Sahara algérien). Bull Soc Zool Fr, 145 (4),383–400.https://societe-zoologique.fr/sites/default/files/revue/2021 01/SZF145%284%29CHEDAD.pdf

[10] Chen, K., Wang, J., Zhang, Z. (2025). Analysis of spatiotemporal evolution and driving factors of ecological environment quality in the Ili-Balkhash Lake Basin in Central Asia. Sci Rep, 15, 22190. https://doi.org/10.1038/s41598-025-06085-8.

[11] Zhang, J., Ding, J., Wu, P. (2020). Assessing arid Inland Lake Watershed Area and Vegetation Response to Multiple Temporal Scales of Drought Across the Ebinur Lake Watershed. Sci Rep, 10, 1354. https://doi.org/10.1038/s41598-020-57898-8.

[12] Hakim, A. R., Riani, E. & Susanti, E. (2025). Floating treatment wetland enhanced with nanobubbles aeration system for nitrogen removal as a sustainable domestic wastewater treatment. Journal of Ecological Engineering, 26(12), 43–54. https://doi.org/10.12911/22998993/208370.

[13] Tiwari, R., & Mahalpure, G. S. (2025). A Detailed Review of pH and its Applications. Journal of Pharmaceutical and Biopharmaceutical Research, 6(2), 492-505. https://doi.org/10.25082/JPBR.2024.02.001.

[14] Corwin, D.L., Yemoto, K. (2020). Salinity: Electrical conductivity and total dissolved solids. Soil Sci Soc Am J, 84, 1442–1461. https://doi.org/10.1002/saj2.20154.

[15] Wei, Y., Jiao, Y., An, D., Li, D., Li, W., & Wei, Q. (2019). Review of Dissolved Oxygen Detection Technology: From Laboratory Analysis to Online Intelligent Detection. Sensors, 19(18), 3995. https://doi.org/10.3390/s19183995.

[16] Saher, F.I., Dalia, M.E. (2017). Metrological evaluation of prepared turbidity working standard solutions to achieve traceability for textile waste water effluents. Egypt. J. Chem, 60(4), 563- 575. https://doi.org/10.21608/ejchem.2017.938.1046.

[17] Utomo, W. P., Wu, H., Ng, Y. H. (2023). Quantification methodology of ammonia produced from electrocatalytic and photocatalytic nitrogen/nitrate reduction. Energies, 16(1), 27. https://doi.org/10.3390/en16010027.

[18] Sarmanov, A., Matela, M., Sultanov, Y. (2024). Salinisation effects on benthic invertebrate assemblages in shallow lakes in arid and semiarid climate zones. Sci Rep, 14, 30622. https://doi.org/10.1038/s41598-024-82527-z.

[19] Abalasei, M.E., Toma, D., Dorus, M., Teodosiu, C. (2025). The impact of climate change on water quality: a critical analysis. Water, 17(21), 3108. https://doi.org/10.3390/w17213108.

[20] Kakabayev, A., Yessenzholov, B., Khussainov, A., Rodrigo-Ilarri, J., Rodrigo-Clavero, M. E., Kyzdarbekova, G., Dankina, G. (2023). The Impact of Climate Change on the Water Systems of the Yesil River Basin in Northern Kazakhstan. Sustainability, 15(22), 15745. https://doi.org/10.3390/su152215745.

[21] Liang, Y., Zhu, H., Bañuelos, G., Yan, B., Zhou, Q., Yu, X., Cheng, X. (2017). Constructed wetlands for saline wastewater treatment: A review. Ecol Eng, 98, 275-85. https://doi.org/10.1016/j.ecoleng.2016.11.005.

[22] Brandon, W., Kerns, S., Chen, S. (2021). Impacts of Precipitation–Evaporation–Salinity coupling on upper ocean stratification and momentum over the tropical pacific prior to onset of the 2018 El Niño. Ocean Model, 168, 1463-5003. https://doi.org/10.1016/j.ocemod.2021.101892.

[23] Li, B., Yang, L., Song, X., Diamantopoulos, E. (2023). Identifying surface water and groundwater interactions using multiple experimental methods in the riparian zone of the polluted and disturbed Shaying River, China. Sci Total Environ., 875, 162616. https://doi.org/ 10.1016/j.scitotenv.2023.162616.

[24] Nachshon, U. (2018). Cropland soil salinization and associated hydrology: trends, processes and examples. Water, 2018, 10(8), 1030. https://doi.org/10.3390/w10081030.

[25] Cui, G., Liu, Y., Li, X., Wang, S., Qu, X., Wang, L., Tong, S., Zhang, M., Li, X., Zhang, W. (2025). Impacts of groundwater storage variability on soil salinization in a semi-arid agricultural plain. Geoderma, 454, 117162. https://doi.org/10.1016/j.geoderma.2024.117162.

[26] Boumaraf, W., Djamai, R., Djabali, N. (2017). Hydro-chemical characterization of an aquatic ecosystem water of El Kala national park (Case of Oubeira Lake, Northeast Algeria). Int J Biosci, 11(1), 59-67. https://doi.org/10.12692/ijb/11.1.59-67.

[27] Mainali, J., Chang, H. (2021). Environmental and spatial factors affecting surface water quality in a Himalayan Watershed, Central Nepal. J Environ Sustain, 9, 100096. https://doi.org/ 10.1016/j.indic.2020.100096.

[28] Al-Rosyid, L., Komarayanti, S., Arifin, P.R., Guritno, W. (2024). Bioremediation of fishery waste using water Lettuce (Pistia stratiotes L.). Ecol Chem Eng S, 2024, 31(3), 329-338. https://doi.org/10.2478/eces-2024-0022.

[29] Dąbrowski, W., Bagińska-Kretowicz, S. & Malinowski, P. (2025). Preliminary studies on the possibility of recovering water from wastewater using constructed wetlands. Journal of Ecological Engineering, 26(8), 57–66. https://doi.org/10.12911/22998993/203662.

[30] Mojumdar, E.H., Sparr, E. (2021). The Effect of pH and salt on the molecular structure and dynamics of the skin. Colloids Surf B Biointerfaces, 198, 111476. https://doi.org/ 10.1016/j.colsurfb.2020.111476.

[31] Cheng, X., Li, Y., Zhang, H., Wang, J., Liu, Q. (2020). Saline and alkaline tolerance of wetland plants under combined stress conditions. Sustainability, 12(5), 1913. https://doi.org/ 10.3390/su12051913.

[32] Mahi, T., Meddour, R., Boulakoud, T. (2016). Soil characteristics and plant distribution in saline wetlands of Oued Righ, northeastern Algeria. Afr J Ecol., 54(3, :312-23. https://doi.org/10.1111/aje.12286.

[33] Zhang, D., Qi, Q., Wang, X., Tong, S., An, Y. (2019). Eco-physiological responses of Carex schmidtii to soil salinization in a semi-arid wetland. Pol J Environ Stud, 28(5), 4009-15. https://doi.org/10.15244/pjoes/94013.

[34] Benslimane, M., Samraoui, B., Samraoui, F. (2021). Does salinity influence the diversity and structure of the wintering waterbirds of Saharan wetlands in Algeria? Arxius de Miscel·lània Zoològ, 19, 135-52. https://doi.org/10.32800/amz.2021.19.0135.

[35] Leberger, R., Geijzendorffer, I.R., Gaget, E., Gwelmami, A., Galewski, T., Pereira, H.M., Guerra, C.A. (2020). Mediterranean wetland conservation in the context of climate and land cover change. Reg Environ Change, 20(67), 1-11. https://doi.org/10.1007/s10113-020-01655-0.

[36] Herbert, E.R., Boon, P., Burgin, A.J., Neubauer, S.C., Franklin, R.B., Ardon, M., Hopfensperger, K.N., Lamers, L.P., Gell, P. (2015). A global perspective on wetland salinization: Ecological consequences of a growing threat to freshwater wetlands. Ecosphere, 6(10), 206. https://doi.org/10.1890/ES14-00534.1.

[37] Li, Y., Yao, G., Li, S., Dong, X. (2025). Predicting and mapping of soil organic matter with machine learning in the black soil region of the southern northeast plain of China. Agronomy, 15(3), 533. https://doi.org/10.3390/agronomy15030533.

[38] Ugya, A. Y. & Meguellati, K. (2022). Modelling Assisted Phytoremediation of Landfill Leachate Using Surface Flow Constructed Wetland Enhanced by Pistia stratiote and Salvinia molesta. Journal of Ecological Engineering, 23(5), 226–236. https://doi.org/10.12911/22998993/147432.

[39] Alsaleh, A.R.S., Alcibahy, M., Abdul Gafoor, F., Al Hashemi, H., Athamneh, B., Al Hammadi, A.A., Seneviratne, L., Al Shehhi, M.R. (2025). Estimation of soil organic carbon in arid agricultural fields based on hyperspectral satellite images. Geoderma, 453, 117151. https://doi.org/10.1016/j.geoderma.2024.117151.

[40] Wang, R., Quan, Y., Zheng, S. & Zhang, X. (2022). Effect of different plant monocultures on nitrogen removal performance in wetland microcosms. Journal of Ecological Engineering, 23(9), 241–249. https://doi.org/10.12911/22998993/151094.

[41] Zhou, Z., Wang, S., Zhao, M., Zhi, F. (2023). Research on art design of urban wetland park planning based on the concept of sustainable development. Ecol Chem Eng S, 30(2), 175-181 https://doi.org/10.2478/eces-2023-0017.

[42] Liang, X., Jian, Z., Tan, Z., Dai, R., Wang, H., Wang, J., Qiu, G., Chang, M., Li, T. (2024). Dissolved oxygen concentration prediction in the pearl river estuary with deep learning for driving factors identification: temperature, pH, conductivity, and ammonia nitrogen. Water, 16(21), 3090. https://doi.org/10.3390/w16213090.

[43] Arliyani, I., Tangahu, B. V. & Mangkoedihardjo, S. (2021). Performance of Reactive Nitrogen in Leachate Treatment in Constructed Wetlands. Journal of Ecological Engineering, 22(5), 205–213. https://doi.org/10.12911/22998993/135314.

[44] Mrkva, L., Schöl, A., Janský, B. (2024). A water quality model for the Czech part of the river Elbe. Ecol Chem Eng S, 31(3), 329-338. https://doi.org/10.2478/eces-2024-0030.

[45] Larance, S., Wang, J., Delavar, M.A., Fahs, M. (2025). Assessing water temperature and dissolved oxygen and their potential effects on aquatic ecosystem using a SARIMA Model. Environments, 12(1), 25. https://doi.org/10.3390/environments12010025.

[46] Masmoudi, T., Benakcha, M., Abdennour, M.A., Bouzekri, A., Amrane, A., Alcala, F.J. (2024). Groundwater quality evaluation for drinking and agricultural purposes. A case study in semi-arid region (Zab El-gharbi SE-Algeria). Desal. Water Treat, 319, 100476. https://doi.org/10.1016/j.dwt.2024.100476.

[47] Zhong, H., Peng L., Xin, Xu., Maoting, Ma., Chengjun Z., Lianfeng, Du., Xuan G. (2025). Spatial distribution and driving factors of nitrogen cycle genes in urban landscape lake. Sustainability, 17(1), 186. https://doi.org/10.3390/su17010186.

[48] Savic, R., Stajic, M., Blagojević, B., Bezdan, A., Vranesevic, M., Nikolić Jokanović, V., Baumgertel, A., Bubalo Kovačić, M., Horvatinec, J., Ondrasek, G. (2022). Nitrogen and Phosphorus Concentrations and Their Ratios as Indicators of Water Quality and Eutrophication of the Hydro-System Danube–Tisza–Danube. Agriculture, 12(7), 935. https://doi.org/10.3390/agriculture12070935.